Check for updates

Received: 12 June 2023 | Accepted: 30 October 2023

DOI: 10.1002/aur.3062

RESEARCH ARTICLE

Prolonged neural encoding of visual information in autism

Gianluca Marsicano[1,2,3] | Luca Casartelli[4] | Alessandra Federici[5] | Sara Bertoni[6,7] | Lorenzo Vignali[8] | Massimo Molteni[4] | Andrea Facoetti[7] | Luca Ronconi[3,9]

[1]Department of Psychology, University of Bologna, Bologna, Italy

[2]Centre for Studies and Research in Cognitive Neuroscience, University of Bologna, Cesena, Italy

[3]Division of Neuroscience, IRCCS San Raffaele Scientific Institute, Milan, Italy

[4]Child Psychopathology Department, Theoretical and Cognitive Neuroscience Unit, Scientific Institute IRCCS E.MEDEA, Bosisio Parini, Italy

[5]MoMiLab, IMT School for Advanced Studies Lucca, Lucca, Italy

[6]Department of Human and Social Sciences, University of Bergamo, Bergamo, Italy

[7]Developmental and Cognitive Neuroscience Lab, Department of General Psychology, University of Padua, Padova, Italy

[8]MED-EL, Innsbruck, Austria

[9]School of Psychology, Vita-Salute San Raffaele University, Milan, Italy

Correspondence
Luca Ronconi, Division of Neuroscience, IRCCS San Raffaele Scientific Institute, Milan 20132, Italy; School of Psychology, Vita-Salute San Raffaele University, Milan, Italy.
Email: ronconi.luca@unisr.it

Abstract

Autism spectrum disorder (ASD) is associated with a hyper-focused visual attentional style, impacting higher-order social and affective domains. The understanding of such peculiarity can benefit from the use of multivariate pattern analysis (MVPA) of high-resolution electroencephalography (EEG) data, which has proved to be a powerful technique to investigate the hidden neural dynamics orchestrating sensory and cognitive processes. Here, we recorded EEG in typically developing (TD) children and in children with ASD during a visuo-spatial attentional task where attention was exogenously captured by a small (zoom-in) or large (zoom-out) cue in the visual field before the appearance of a target at different eccentricities. MVPA was performed both in the cue-locked period, to reveal potential differences in the modulation of the attentional focus, and in the target-locked period, to reveal potential cascade effects on stimulus processing. Cue-locked MVPA revealed that while in the TD group the pattern of neural activity contained information about the cue mainly before the target appearance, the ASD group showed a temporally sustained and topographically diffuse significant decoding of the cue neural response even after the target onset, suggesting a delayed extinction of cue-related neural activity. Crucially, this delayed extinction positively correlated with behavioral measures of attentional hyperfocusing. Results of target-locked MVPA were coherent with a hyper-focused attentional profile, highlighting an earlier and stronger decoding of target neural responses in small cue trials in the ASD group. The present findings document a spatially and temporally overrepresented encoding of visual information in ASD, which can constitute one of the main reasons behind their peculiar cognitive style.

Lay Summary

This study unveils how incoming visual input is encoded at the neural level in children with autism spectrum disorder (ASD), and how this encoding impacts on their attentional selection. Using multivariate pattern analysis (MVPA) of high-resolution EEG data, we show that children with ASD exhibit a temporally prolonged and topographically broader overrepresentation of visual information, as compared to their typically developing peers. Such excessive stimulus encoding could in turn lead to difficulties in reorienting attentional resources to subsequent relevant incoming stimuli, leading to their peculiar hyperfocused attentional profile. This study not only provides new evidence about important neural mechanisms of visual information processing in ASD, but it also shows that MVPA approaches can detect neural dynamics that may remain otherwise largely blind to other univariate analyses approaches.

This is an open access article under the terms of the Creative Commons Attribution-NonCommercial-NoDerivs License, which permits use and distribution in any medium, provided the original work is properly cited, the use is non-commercial and no modifications or adaptations are made.
© 2023 The Authors. *Autism Research* published by International Society for Autism Research and Wiley Periodicals LLC.

KEYWORDS
autism spectrum disorders, EEG, multivariate pattern analysis, visual attention, visual processing

INTRODUCTION

Autism spectrum disorder (ASD) is a multi-factorial neurodevelopmental disorder characterized by a heterogeneous spectrum of significant impairments in sensory, cognitive, and social domains, affecting about 1% of the population (Hyman et al., 2020; Lai et al., 2020).

In line with the neuro-constructivist theoretical framework (Farran & Karmiloff-Smith, 2011; Johnson, 2011; Karmiloff-Smith, 1998), a large body of findings have highlighted that low-level dysfunctions in the visual attentional domain might represent the core deficits underlying the impairments in high-level social and communicative abilities (Elsabbagh et al., 2011; Mottron et al., 2006). A widely documented attentional anomaly in ASD is their hyper-focusing of visuo-spatial attention, which is linked to difficulties in disengagement visuo-spatial attentional resources (Lawson et al., 2017; Lieder et al., 2019; Noel et al., 2021), potentially impacting global visual analysis and the correct development of joint attention skills (Burack, 1994; Guy et al., 2019; Mann & Walker, 2003; Ronconi et al., 2013, 2018). However, the neural dynamics underlying this inflexible and hyper-focused visual attentional style in ASD population remain poorly understood. Multivariate pattern analysis (MVPA) of EEG data is a particularly promising method to investigate the fast and transient neural dynamics orchestrating attentional processes (Battistoni et al., 2020; Marti & Dehaene, 2017; Moerel et al., 2022; Munneke et al., 2021). Recently, MVPA has proven to be a powerful methodological tool to unveil the hidden dysfunctional neural dynamics underlying anomalies in different cognitive domains (Bae et al., 2020; Farran et al., 2020; Li et al., 2023). Accordingly, MVPA could be used to deepen the understanding of visuo-spatial attentional anomalies in children with ASD for several reasons.

First, the nature of the neuroelectrical EEG activity is intrinsically multivariate, structuring itself as a complex signal characterized by spatio-temporal features (Mitra & Pesaran, 1999). Univariate analyses of the EEG signal are based on a hypothesis-driven approach, implying the need to define a priori the temporal windows (*which time-points*?) and the spatial location (*which electrodes*?) of interest, constraining the analysis to the investigation of the differences across group or conditions identified in components of the neural signal with a known meaning (e.g., ERPs), leading to the possibility of excluding relevant information or to incur into the reverse inference problem (Poldrack, 2006, 2011; Sinnott-Armstrong & Simmons, 2021). On the contrary, MVPA allows to analyze the EEG signal with minimal a priori hypotheses regarding the temporal and spatial dimensions. This allows investigators to evaluate the differences in the patterns of neural activity elicited by different experimental conditions from the whole scalp in its entire time course (Fahrenfort et al., 2017, 2018), providing greater sensitivity to detect characteristics of the neural activity representing specific patterns of information processing which remain largely blind to univariate techniques (Grootswagers et al., 2017; Marti & Dehaene, 2017).

Second, and most relevant to the current study, recent evidence has demonstrated a greater efficacy of the MVPA of EEG data in identifying hidden neural dynamics exhibited by individuals with neurodevelopmental (Williams Syndrome: Farran et al., 2020; ADHD: Li et al., 2023) and psychiatric (Schizophrenia: Bae et al., 2020) disorders. Indeed, for populations in which the observed behavior is the result of an alternative developmental pathway, potentially supported by distinct neural mechanisms, a multivariate approach may provide a more explanatory understanding of their sensory and cognitive profile. Hence, MVPA could be seen as a natural candidate in the analysis of the EEG activity of individuals with ASD, whose neural activity profiles are difficult to predict given the high inter-individual heterogeneity within the ASD spectrum (Masi et al., 2017; Uljarević et al., 2017).

At present, the application of this multivariate approach to uncover the neural dynamics underlying visuo-spatial attentional processes in the ASD population is not documented. In the current study, we aimed to implement an MVPA approach to investigate the hidden neural dynamics underlying visual attentional mechanisms in ASD. To this end, the EEG signal was acquired in a sample of typically developing (TD) children and children with ASD during a visual attentional task capable of probing the exogenous attentional focusing abilities, where a small (zoom-in) or a large (zoom-out) circular cues preceded the appearance of visual targets (a dot) at different eccentricities. Using this and other similar paradigms it has been shown that the enlargement of visuo-spatial attentional focus in children with ASD is delayed as compared to TD children, suggesting an atypical hyper-focusing of visuo-spatial attention (Burack, 1994; Mann & Walker, 2003; Ronconi et al., 2013, 2018). We computed MVPA of EEG data both in cue- and target-locked time windows, with the aim to compare neural patterns elicited during the modulation of the attentional focus and after the appearance of the target presented under different attentional regimes. Two types of MVPA analyses were employed to describe how incoming visual input is encoded at the neural level in children with ASD, and how this encoding impacts on attentional capture (please, see method section). Furthermore, this procedure allowed us to

19393806, 2024, 1, Downloaded from https://onlinelibrary.wiley.com/doi/10.1002/aur.3062 by CochraneItalia, Wiley Online Library on [07/07/2024]. See the Terms and Conditions (https://onlinelibrary.wiley.com/terms-and-conditions) on Wiley Online Library for rules of use; OA articles are governed by the applicable Creative Commons License

disentangle to what extent neural processing of visual information extends over time in ASD and TD groups.

Following previous evidence demonstrating a sustained hyper-focusing of visual attention in children with ASD (e.g., Ronconi et al., 2013, 2018), and a difficulty in disengagement their visual resources (Geurts et al., 2009; Noel et al., 2021), it is conceivable that ASD group may show atypical patterns of neural activation, characterized by a prolonged information processing and by an over-representation of visual information, in both cue- and target-locked time windows.

MATERIALS AND METHODS

Participants

Study participants were 19 children with ASD (18 M; 1 F; mean age: 11.21 ± 1.99) and 20 TD children (16 M; 4 F; mean age: 11.25 ± 1.55) recruited at the Developmental Psychopathology Unit of the "E. Medea" Scientific Institute (Bosisio Parini, Italy). Patients included in the ASD group were diagnosed by expert clinician according to the DSM-IV criteria (American Psychiatric Association, 1994) and to the score assessed by Autistic Diagnosis Observation Scale (Lord et al., 2002). Moreover, they were selected according to the following criteria: (1) full-scale IQ > 70 measured by the WISC-III (Wechsler, 1993); (2) absence of drug therapy; (3) absence of major behavioral problems; (4) absence of Attentional Deficit Hyperactivity Disorder and Developmental Dyslexia (American Psychiatric Association, 1994); (5) normal/corrected-to-normal vision and normal hearing. Children of the TD group were recruited in schools in the same geographical area. According to the parents' report, TD children did not have prior history of any psychiatric disorders. Cognitive level was estimated with two verbal subtests (vocabulary and similarities) and two performance subtests (block design and image completion) of WISC-III (Wechsler, 1993; please, see Table 1 for a detailed description). The entire research protocol was approved by the ethics committees of the I.R.C.C.S. "E. Medea." Informed consent was obtained from each child and their parents.

Stimuli and procedure

The *visual attentional task* (Figure 1) began after placement of the EEG cap. All stimuli were middle gray displayed on a black background. Each trial started with the onset of a central fixation point (0.5°) that participants were instructed to fixate throughout the trial. After 500 ms, a non-informative small or large circular focusing cue was presented, anticipating with equal probability the target appearance (20 ms) in a central or peripheral locations. In the small cue condition, a circle with a ray of 4° was presented concentrically to the fixation point. In the large cue condition, a circle with a ray of 12.5° was presented concentrically to the fixation point. The target stimulus was a point of 0.5° which could appear at one of the two possible distances from the fixation point on the horizontal axis (i.e., 2 ad 12°). Considering that the main aim of the present study was to measure the time-course of EEG activity during different attentional states, the cue-target SOA was set for the vast majority of trials to 500 ms. A smaller portion of trials (64/624 about 10%) with a cue-target SOA of 100 ms was also presented in order to avoid participants developing a strong prediction about the timing of target appearance. Participants were instructed to press the spacebar on the keyboard as fast as possible after the target onset, and the computer recorded RTs within 2 s from the stimulus onset. At the end of each trial, a blank screen appeared for 1500 ms and then a new trial began. The experimental session consisted of 624 randomized trials (SOA 500 ms: 2 cue size × 2 eccentricity × 2 spatial positions of target presentations × 70 repetitions; SOA 100 ms: 64 four trials: 2 cue size × 2 eccentricity × 2 spatial positions of target presentations × 8 repetitions).

Behavioral analysis

We performed a mixed analysis of variance (ANOVA) on the mean of reaction times (RTs) with a 2 × 2 × 2 design in which within-subject factors were the focusing cue-size (two levels: small and large) and eccentricity of the target (eccentricity 2 and eccentricity 12), while the between-subject factor was the group (ASD and TD). All post-hoc comparisons were performed with Bonferroni correction. Furthermore, although the visuo-attentional task implemented in the current study was quite simple, as a control analysis we performed a mixed ANOVA on the mean of Hit Rates with the same 2 × 2 × 2 design.

EEG data and preprocessing

EEG was recorded with 64 Ag/AgCl electrodes (Hydrocel Geodesic Sensor Net, Inc.) during the execution of the task. Data were sampled online at 500 Hz. During recording, the reference channel was Cz. Offline, data were downsampled to 250 Hz, recomputed to an average reference, bandpass filtered between 0.05 and 80 Hz using Butterworth filters, and notch filtered to remove 50-Hz line noise. To analyze the EEG activity elicited by the cue (i.e., attentional condition decoding; cue-locked) and target (i.e., target location decoding; target locked), data were segmented between −500 and +1000 ms relative to the cue onset and between −200 and +500 ms relative to the target onset. In both cases, a 200 ms pre-stimulus window was used as baseline. We computed the Independent Component Analysis (ICA) to identify and remove ocular artifacts for each subject. As an additional check, we quantified the ocular artifacts

19393806, 2024, 1, Downloaded from https://onlinelibrary.wiley.com/doi/10.1002/aur.3062 by CochraneItalia, Wiley Online Library on [07/07/2024]. See the Terms and Conditions (https://onlinelibrary.wiley.com/terms-and-conditions) on Wiley Online Library for rules of use; OA articles are governed by the applicable Creative Commons License

TABLE 1 Descriptive statistics for ASD and TD groups (first and second columns). Statistical comparisons (independent sample *t*-tests) between groups for each test (third column).

	ASD ($N = 19$, 18 M), mean (SD)	TD ($N = 20$, 16 M), mean (SD)	*p*-value (independent sample *t*-test)
Age	11.21 (±1.99)	11.25 (±1.55)	n.s
TIQ	102.11 (±16.77)	—	—
WISC III – Vocabulary	9.37 (±2.85)	12.10 (±2.29)	0.004
WISC III – Similarities	10.74 (±2.42)	12.10 (±2.29)	n.s
WISC III – Block design	11.95 (±3.96)	12.35 (±3.10)	n.s
WISC III – Picture completion	11.74 (±2.68)	11.95 (±2.65)	n.s
Social Communication Questionnaire (SCQ) – Current	12.00 (±6.60)	4.75 (±3.08)	<0.001
Social Communication Questionnaire (SCQ) – Lifetime	20.58 (±6.87)	4.55 (±2.21)	<0.001
ADOS – Communication	2.79 (±1.44)	—	—
ADOS – Social interaction	6.79 (±2.44)	—	—

Abbreviations: ASD, autism spectrum disorder; TD, typically developing; n.s., non significant ($p>0.05$).

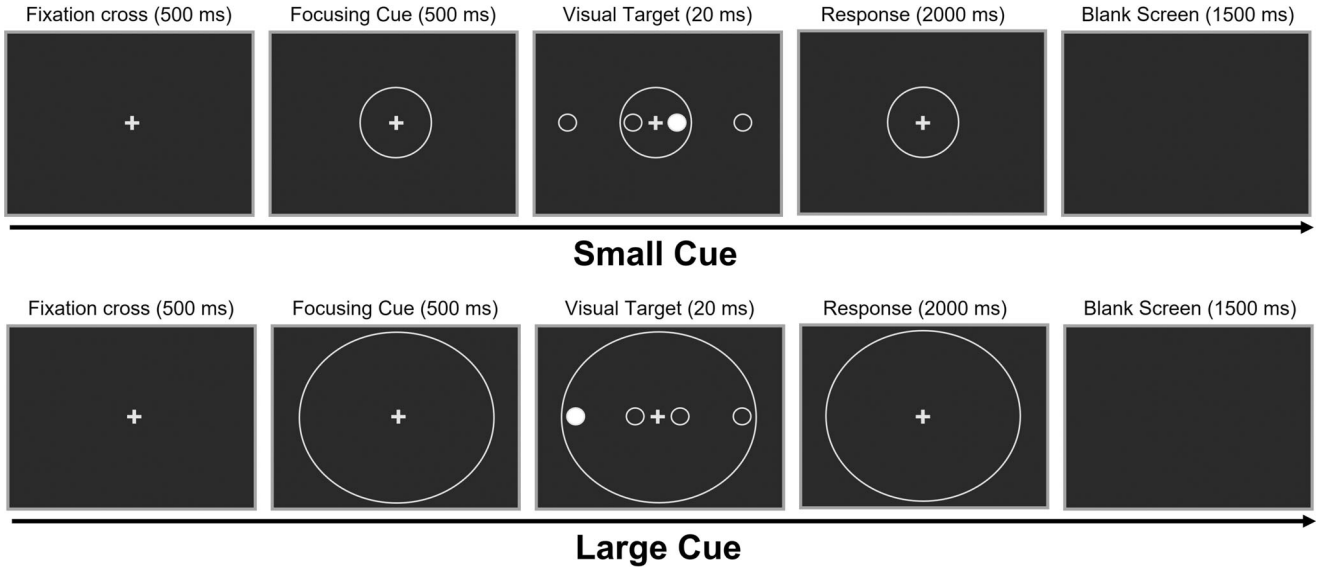

FIGURE 1 Schematic representation of the visual attentional task. Each trial began with the presentation of a central fixation cross (500 ms), followed by a non-informative small (small cue trials; zoom-in; upper panel) or a large (large cue trials; zoom-out; lower panel) circular cues (500 ms) preceding the appearance of visual targets (white point; 20 ms) delivered at different eccentricities from central fixation cross (central, 2° from fixation; peripheral, 12° from fixation). In a smaller portion of trials, the circular cue appeared for 100 ms to avoid participants developing a strong prediction about the timing of target appearance (64/624 trials). At the target onset, participants were instructed to press the spacebar on the keyboard as fast as possible (2000 ms). At the end of each trial a blank screen appeared for 1500 ms and then a new trial began.

(EOG) present in the EEG signal for each participant and each condition (i.e., cue-locked and target locked analysis; please, see below). The independent samples *t*-test comparisons between ASD and TD groups showed no significant difference in EOG artifacts in any of the experimental conditions (all ps >0.358). For the cue-locked analysis, the total number of artifacts-free epochs used for statistical analysis was 545.10 ± 53.95 for ASD group and 519.05 ± 45.80 for TD groups. For target-locked analysis, the total number of trials used was 252.64 ± 49.12 for ASD group and 266.72 ± 24.12 for TD group (please, see supplementary for a more detailed description).

All the pre-processing steps were carried out using the EEGLAB toolbox functions (Delorme & Makeig, 2004) in MATLAB R2019a.

MVPA analysis – diagonal decoding

MVPA was implemented using ADAM (Amsterdam Decoding and Modeling Toolbox; Fahrenfort et al., 2018)

19393806, 2024, 1, Downloaded from https://onlinelibrary.wiley.com/doi/10.1002/aur.3062 by CochraneItalia, Wiley Online Library on [07/07/2024]. See the Terms and Conditions (https://onlinelibrary.wiley.com/terms-and-conditions) on Wiley Online Library for rules of use; OA articles are governed by the applicable Creative Commons License

on MATLAB, in both the cue- and target-locked time windows, separately for ASD and TD groups, with the aim to compare neural patterns elicited by (i) different cue size (large vs. small); (ii) different target presentation conditions in large cue trials: eccentricity 2 vs. eccentricity 12; (iii) different target presentation conditions in small cue trials: eccentricity 2 vs. eccentricity 12. In a first step, we performed diagonal decoding, where the classifier was trained and tested on the same timepoints.

In detail, standard linear discriminant analysis (LDA) was performed for all comparisons of these experimental conditions at each time point, using a 10-fold cross-validation procedure that considered data from all the electrodes. Classification performance was measured using the area under the curve (AUC) and tested against chance (50%) to judge the timepoints at which the classifier was successfully able to differentiate between experimental conditions, using right-sided cluster-based permutation t-tests with 2500 iterations (above chance = 0.5; Maris & Oostenveld, 2007). Furthermore, we computed topographical maps based on classifier weights for individual features for each comparison (Haufe et al., 2014).

In addition, following scalp maps distribution of diagonal decoding and previous neuroimaging studies highlighting the role of different brain regions in attentional focusing mechanisms (e.g., Belmonte et al., 2010; Ruff et al., 2008), we decided to compute the decoding analysis described above separately for different cluster of neighboring electrodes (i.e., Region of Interest; ROIs), dividing anterior, central and posterior scalp areas each into 3 different ROIs (i.e., left, central and right). This procedure allowed us to have a complete picture of all scalp locations (see Figure S1).

All individual decoding measures were inspected before computing statistical analyses to test for potential outliers (i.e., Grubbs' test, ESD method, extreme studentized deviate; $p > 0.05$; see single subject decoding measures in supplementary).

In addition, similarly to some recent studies (Bae et al., 2020; Farran et al., 2020; Li et al., 2023; Mares et al., 2020), we analyzed different key decoding parameters that allow a deeper investigation of the neural activation profiles differences associated with the discrimination of the experimental classes between ASD and TD groups. These parameters, which were tested using independent sample *t*-tests, are: (i) decoding onset, that is, the first timepoint at which decoding becomes significant; (ii) decoding sustainability, that is, the percentage of significant timepoints decoded over time; (iii) decoding peak, that is, the highest decoding accuracy value (AUC); (iv) decoding peak latency, that is, the timepoint at which accuracy (AUC) is highest.

MVPA analysis – time generalization

We performed a temporal generalization analysis using cross-classification across time (King & Dehaene, 2014) in the cue-locked time window (i.e., attentional condition decoding), with the aim to disentangle whether the neural patterns elicited by the cue-size were sustained and generalized even after the onset of the target. Temporal generalization offers a way to visualize the dynamics of activity present in the signal by testing how well training for each individual timepoint extends to successful classification for the other timepoints within the signal, allowing to evaluate whether the neural responses identified at given timepoints are generalized at other timepoints. Temporal generalization measures used the same methods as described for the MVPA diagonal decoding analysis, but with repeated testing for each time point and 2500 iterations of cluster-based permutations.

Correlations between attentional condition decoding and behavioral measures

To investigate potential relationships between the patterns of neural activity elicited by the cues and the behavioral responses at the target, we performed Pearson correlation. In detail, this analysis was planned post-hoc, to investigate whether the participants' behavioral responses in large and small cue trials at different target eccentricities (i.e., 2 and 12) was influenced by an increased decoding activity elicited by the cue after the target appearance. To this aim, the decoding accuracy from all electrodes after the target onset (500–998 ms) was correlated with the RTs in zoom-in and zoom-out conditions. Multiple comparisons were corrected using Bonferroni correction.

Univariate ERPs analysis

Alongside MVPA analysis, with the aim to explore potential differences in the observed effects between univariate (i.e., ERPs) and MVPA techniques of EEG data, we performed univariate ERPs analyses both in cue- and target-locked time windows. Cue- and target-locked ERPs components were identified based on previous literature that investigated the neuroelectric correlates of attentional zooming mechanisms in the TD population (Luo et al., 2001; Fu et al., 2005; Song et al., 2006; Zhang et al., 2018), through visual inspection of the ERPs waveform and topographical scalp maps. Following previous studies, to investigate the modulation of early visual evoked potentials by the scale effect of the spatial attention, P1 and N1 components were calculated, choosing, respectively, time windows of 100–150 ms and 200–250 ms after cue onset (cue-locked analysis; large vs. small cue) and time windows of 140–190 ms and 220–270 ms after target onset (target-locked analysis; target location following large vs. small cue trials). These analyses were computed on the central posterior ROI (for a graphical representation, see Supplementary Figure 2), which was the most representative clusters of electrodes to investigate ERPs components associated to cue-size

19393806, 2024, 1, Downloaded from https://onlinelibrary.wiley.com/doi/10.1002/aur.3062 by CochraneItalia, Wiley Online Library on [07/07/2024]. See the Terms and Conditions (https://onlinelibrary.wiley.com/terms-and-conditions) on Wiley Online Library for rules of use; OA articles are governed by the applicable Creative Commons License

modulation, based on previous literature (Luo et al., 2001; Fu et al., 2005; Song et al., 2006; Zhang et al., 2018) and to visual inspection of topographical scalp maps. Regarding cue-locked analysis, we performed separated repeated measures ANOVA on the peak latency and mean amplitude, separately, of P1 and N1 components with the aim of testing whether ERPs modulations are influenced by the Cue-Size (within-subjects factor: large and small), using as between-subjects factor the Group (ASD and TD). Regarding target-locked analysis, we performed separated repeated measures ANOVA on the peak latency and mean amplitude, separately, of P1 and N1 components with the aim of testing whether ERPs modulations were influenced by the cue-size (within-subjects factor: large and small) and eccentricity (within-subjects factor: eccentricity 2 and eccentricity 12), using as between-subjects factor the group (ASD and TD). The Greenhouse–Geisser correction was applied in cases where the sphericity assumption was violated. All post-hoc comparisons were performed with Bonferroni correction.

RESULTS

Behavioral results

The ANOVA on RTs showed a significant main effect of cue-size ($F_{(1,37)} = 6.870$, $p = 0.013$, $\eta 2p = 0.157$) and Eccentricity ($F_{(1,37)} = 6.803$, $p = 0.013$, $\eta 2p = 0.155$). For the cue size, faster RTs emerged for the large cue ($M = 347.67$, SD = 60.33; $p = 0.013$) compared to small cue ($M = 363.95$, SD = 59.93) condition. For eccentricity, faster RTs were observed for Eccentricity 2 ($p = 0.013$; $M = 345.80$, SD = 57.98) compared to Eccentricity 12 ($M = 365.12$, SD = 62.28). The main effect of Group was not significant ($F_{(1,37)} = 3.529$, $p = 0.746$, $\eta 2p = 0.003$) and, in addition, no significant interactions emerged (all p-values >0.088; Supplement Figure S2).

The results showed an effective influence of the attentional conditions (large cue vs. small cue trials) on the overall pattern of RTs, although no RTs differences emerged between TD and ASD groups, differently from previous evidence (Ronconi et al., 2012, 2013, 2018). As expected, the ANOVA on hit rates revealed no significant effects or interactions between factors ($p > 0.448$), revealing no significant differences between groups. In detail, both groups reported similar high hit rates in all conditions analyzed (ASD: M 0.97 ± 0.05; TD: M 0.97 ± 0.03).

Decoding small versus large cue trials: MVPA – diagonal decoding (all electrodes)

Regarding cue-locked analyses (i.e., large vs. small cue trials), first we trained and tested the classifier to investigate potential differences considering all electrodes on the scalp. The cluster-based permutation analysis revealed that classification accuracy (AUC) was sustained significantly above chance level (50%) in both the ASD and TD groups (Figure 2a).

In detail, the cluster-based permutation analysis revealed a significant decoding of experimental conditions ($p < 0.001$; 96–998 ms for the ASD group, and 104–998 ms for the TD group (see Figure 2a). The decoding peak after cue onset emerges earlier in ASD with respect to the TD group (ASD: 156 ms; TD: 168 ms), with the ASD group reaching a higher level of peak decoding accuracy (69.72%) compared to the TD group (66.91%). To evaluate these differences more deeply, the neural activation profiles associated with the pattern of neural activity elicited by the small and large cue between ASD and TD groups, we compared key decoding measures (e.g., Farran et al., 2020; see Table 2 for detailed results description). We observed a significant differences between ASD and TD groups in decoding onset ($t_{(37)} = -2.91$, $p = 0.006$, Cohen's $d = -0.93$; ASD: 156 ± 23.66 ms; TD: 168 ± 99.87 ms), showing an earlier discrimination of experimental conditions examined in the ASD group when compared to TD group.

In addition, we computed cluster-based permutation corrected t-tests to evaluate statistical differences in AUC between ASD and TD groups; this analysis did not show statistically significant differences ($p > 0.05$).

Decoding large versus CUE small trials: MVPA (ROIs – cluster of electrodes)

We investigated the regional differences of the neural patterns elicited by the cue-size, performing the decoding analysis separately for different ROIs (Figure 2c). This analysis revealed, as expected given the different physical dimensions of the cues, that for both groups the highest decoding accuracy (AUC) was evident in the central-posterior ROI (Figure 2c; $p < 0.001$ for both groups). In detail, the ASD group showed both a higher AUC peak and an earlier accuracy peak latency (ASD: AUC = 70.31%, 156 ms) as compared to the TD group (TD: AUC = 66.26%, 160 ms).

Importantly, when looking at the other clusters of electrodes (Figure 2c), we found that only the ASD group showed a spatially diffuse significant decoding that was sustained even after the target onset (500 ms), potentially suggesting atypical information processing and a hyper-focusing of attentional resources. In detail, within-group cluster-based paired-sample t-test analysis revealed that, for both ASD and TD groups, cue-locked neural response was significantly decoded in different spatial scalp areas up to the target onset (500 ms), showing an involvement of anterior, central and posterior regions during modulation of attentional resources. However, only the ASD group showed significant decoding even

19393806, 2024, 1, Downloaded from https://onlinelibrary.wiley.com/doi/10.1002/aur.3062 by CochraneItalia, Wiley Online Library on [07/07/2024]. See the Terms and Conditions (https://onlinelibrary.wiley.com/terms-and-conditions) on Wiley Online Library for rules of use; OA articles are governed by the applicable Creative Commons License

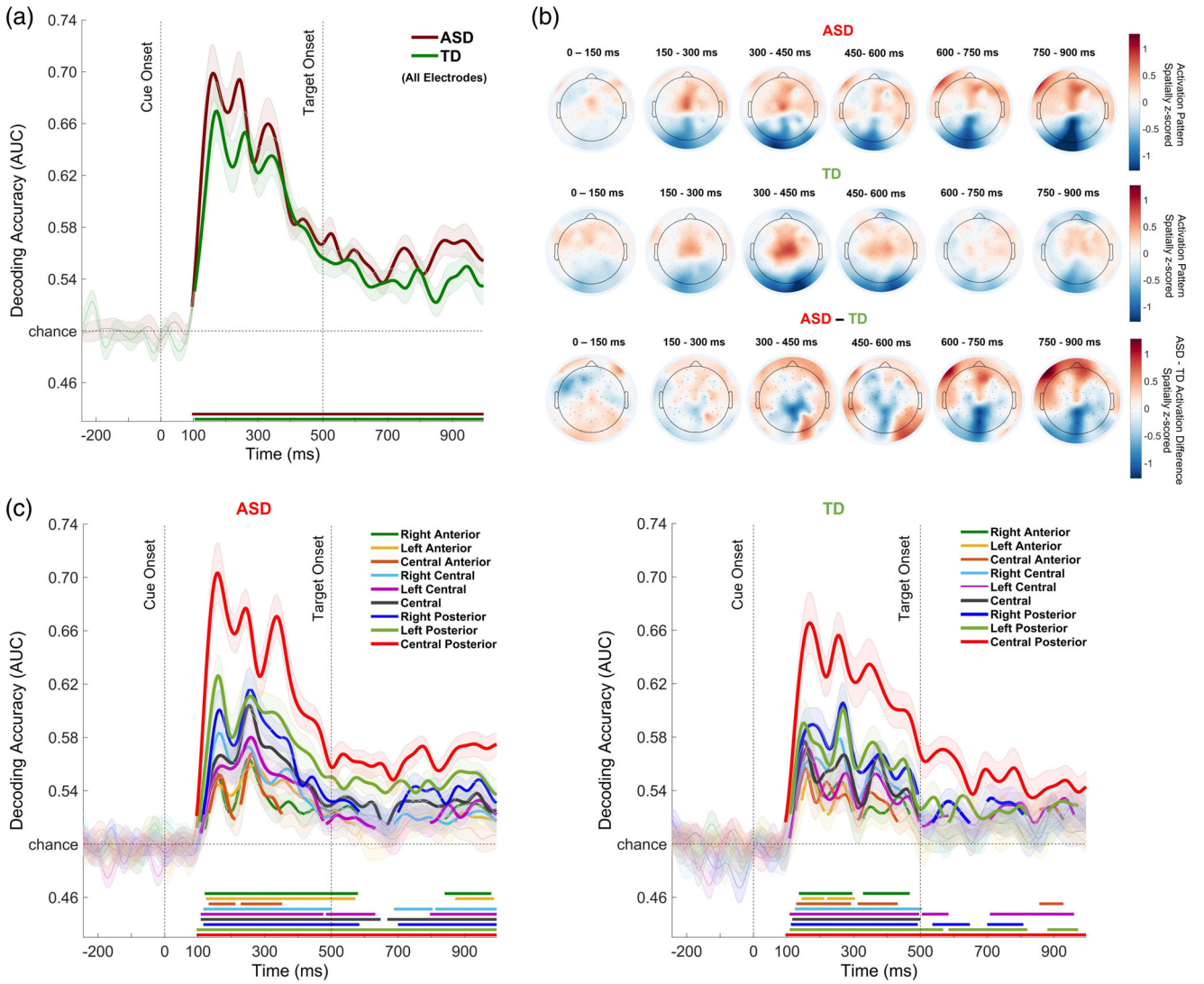

FIGURE 2 Large versus small cue trials diagonal decoding results. (a) The diagonal decoding (on all the electrodes) of the cues neural response (large cue versus small cue trials) revealed that decoding accuracy (AUC) was sustained significantly above chance level (solid lines; 50%) in both the autism spectrum disorder (ASD) (red line) and typically developing (TD) (green line) groups. (b) Activation patterns derived from the product of the weight vectors and the covariance matrix for individual features (electrodes) over cue-locked time window. The resulting topographic maps represented *z*-scores, showing the spatial distribution of the neural activity that underlies successful discrimination between experimental conditions. The upper, middle, and lower panels show topographic maps of the ASD group, the TD group, and the difference between the two groups, respectively. (c) Large versus Small cue trials diagonal decoding performed on nine spatially separate clusters of neighboring electrodes, revealing a spatio-temporally diffuse decoding, with the highest decoding accuracy (AUC) evident in the central-posterior cluster for both groups (ASD and TD). Furthermore, this analysis showed that even after the target onset (vertical dashed line at 500 ms) the ASD group showed a spatially diffuse significant decoding as compared to TD individuals. Vertical lines indicate cue appearance (0 ms) and target onset (500 ms). The horizontal line indicates the chance level (50%) against which the performance was tested to judge at which timepoints the classifier was successfully able to differentiate between experimental conditions (right-sided cluster-based permutation t-tests; $p < 0.05$). Shaded areas around bars represent the standard error across participants.

after target onset in the following ROIs: left posterior, right posterior, left central, central, right central, left anterior and right anterior scalp areas. On the contrary, for the TD group the significance of the decoding expires at the onset of the target, with the exception of the central posterior (following the same trend of significance of ASD group) and the three posterior ROIs. The significance of the posterior ROI after the onset of the target could be explained by the core role played by these areas in modulating attentional focus. Instead, the decoding significance in the left central ROI was identified during the target response time range, potentially reflecting the activity of motor areas that are differentially modulated by the cue size, compatible with the different RTs reported in the two attentional conditions. To thoroughly evaluate the differences between ASD and TD groups we

19393806, 2024, 1, Downloaded from https://onlinelibrary.wiley.com/doi/10.1002/aur.3062 by CochraneItalia, Wiley Online Library on [07/07/2024]. See the Terms and Conditions (https://onlinelibrary.wiley.com/terms-and-conditions) on Wiley Online Library for rules of use; OA articles are governed by the applicable Creative Commons License

TABLE 2 Descriptive statistics for ASD and TD groups and statistical comparisons within and between groups for each MVPA analysis performed (large vs. small cue trials diagonal decoding on all electrodes; large vs. small cue trials diagonal decoding on ROIs; large vs. small cue trials temporal generalization; target location diagonal decoding on all electrodes).

Cue-locked diagonal decoding (all electrodes); large vs. small cue trials			
Key decoding measures	**ASD (paired-sample t-test)**	**TD (paired-sample *t*-test)**	**ASD versus TD between comparisons (*p*-value, independent sample *t*-test)**
Classification accuracy (AUC)	96–998 ms $p < 0.001$ (cluster-based permutation)***	104–998 ms $p < 0.001$ (cluster-based permutation)***	$p > 0.05$ (cluster-based permutation)
Decoding sustainability	0.59 ± 0.03%	0.57 ± 0.04%	$t_{(37)} = 1.46$, $p = 0.47$, Cohen's $d = 0.32$
Decoding peak amplitude	0.76 ± 0.08 (AUC)	0.74 ± 0.07 (AUC)	$t_{(37)} = 0.67$, $p = 0.50$, Cohen's $d = 0.216$
Decoding peak latency	236.64 ± 139.95 ms	232 ± 137.64 ms	$t_{(37)} = 0.099$, $p = 0.13$, Cohen's $d = 0.32$
Decoding onset	156 ± 23.66 ms	168 ± 99.87 ms	$t_{(37)} = -2.91$, $p = 0.006$, Cohen's $d = -0.93$**
Cue-locked diagonal decoding (ROIs); large vs. small cue trials			
ROIs classification accuracy (AUC)	**ASD (paired-sample *t*-test)**	**TD (paired-sample *t*-test)**	**ASD versus TD between comparisons (*p*-value, independent sample *t*-test)**
Right posterior	116–584 ms; 700–996 ms $p < 0.001$ (cluster-based permutation)***	112–492 ms; 536–648 ms; 700–808 ms $p < 0.001$ (cluster-based permutation)***	$t_{(37)} = 0.952$, $p = 0.347$, Cohen's $d = 0.305$
Central posterior	96–998 ms $p < 0.001$ (cluster-based permutation)***	96–998 ms $p < 0.001$ (cluster-based permutation)***	$t_{(37)} = 1.115$, $p = 0.272$, Cohen's $d = 0.357$
Left posterior	96–998 ms $p < 0.001$ (cluster-based permutation)***	108–568 ms; 584–820 ms; 880–972 ms $p < 0.001$ (cluster-based permutation)***	$t_{(37)} = 2.453$, $p = 0.019$, Cohen's $d = 0.786$*
Right central	116–500 ms; 688–804 ms; 812–996 ms $p < 0.001$ (cluster-based permutation)***	124–504 ms; 916–996 ms $p < 0.001$ (cluster-based permutation)***	$t_{(37)} = 0.352$, $p = 0.727$, Cohen's $d = 0.113$
Central	108–648 ms; 668–996 ms $p < 0.001$ (cluster-based permutation)***	116–500 ms $p < 0.001$ (cluster-based permutation)***	$t_{(37)} = 2.031$, $p = 0.049$, Cohen's $d = 0.651$*
Left central	108–476 ms; 484–632 ms; 796–996 ms $p < 0.001$ (cluster-based permutation)***	108–496 ms; 504–584 ms; 708–960 ms $p < 0.001$ (cluster-based permutation)***	$t_{(37)} = -0.365$, $p = 0.717$, Cohen's $d = -0.117$
Right anterior	120–580 ms; 840–980 ms $p < 0.001$ (cluster-based permutation)***	136–296 ms; 328–488 ms $p < 0.001$ (cluster-based permutation)***	$t_{(37)} = 1.645$, $p = 0.109$, Cohen's $d = -0.527$
Central anterior	132–212 ms; 228–352 ms $p < 0.001$ (cluster-based permutation)***	128–292 ms; 312–432 ms; 856–928 ms $p < 0.001$ (cluster-based permutation)***	$t_{(37)} = -0.389$, $p = 0.699$, Cohen's $d = -0.125$
Left anterior	124–572 ms; 872–988 ms $p < 0.001$ (cluster-based permutation)***	144–212 ms; 220–304 ms $p < 0.001$ (cluster-based permutation)***	$t_{(37)} = 0.829$, $p = 0.412$, Cohen's $d = 0.266$
Cue-locked temporal generalization; large vs. small cue trials			
	ASD (paired-sample *t*-test)	**TD (paired-sample *t*-test)**	**ASD versus TD between comparisons (*p*-value, independent sample *t*-test)**
Cue-related neural activity – temporal generalization	156–998 ms $p < 0.001$ (cluster-based permutation)***	ns $p > 0.05$ (cluster-based permutation)	ns $p > 0.05$ (cluster-based permutation)

19393806, 2024, 1, Downloaded from https://onlinelibrary.wiley.com/doi/10.1002/aur.3062 by CochraneItalia, Wiley Online Library on [07/07/2024]. See the Terms and Conditions (https://onlinelibrary.wiley.com/terms-and-conditions) on Wiley Online Library for rules of use; OA articles are governed by the applicable Creative Commons License

TABLE 2 (Continued)

Cue-locked temporal generalization; large vs. small cue trials			
	ASD (paired-sample *t*-test)	**TD (paired-sample *t*-test)**	**ASD versus TD between comparisons (*p*-value, independent sample *t*-test)**
Testing of the cues neural response decoded on the time range around the decoding peak (100–200 ms)	108–998 ms $p < 0.001$ (cluster-based permutation)***	112–491 ms $p < 0.001$ (cluster-based permutation)***	ns $p > 0.05$ (cluster-based permutation)
Target-locked diagonal decoding (all electrodes); Large cue trials based on target eccentricity (2 vs. 12°)			
Key decoding measures	**ASD (paired-sample t-test)**	**TD (paired-sample *t*-test)**	**ASD versus TD between comparisons (*p*-value, independent sample *t*-test)**
Classification accuracy (AUC)	144–496 ms $p < 0.001$ (cluster-based permutation)***	132–496 ms $p < 0.001$ (cluster-based permutation)***	$p > 0.05$ (cluster-based permutation)
Decoding sustainability	56.96 ± 0.29%	55.56 ± 0.33%	$t_{(37)} = 1.39$, $p = 0.17$, Cohen's $d = 0.44$
Decoding peak amplitude	67.74 ± 0.34 (AUC)	66.32 ± 0.32 (AUC)	$t_{(37)} = 1.27$, $p = 0.21$, Cohen's $d = 0.40$
Decoding peak latency	310.94 ± 82.27 ms	221.8 ± 169.23 ms	$t_{(37)} = 1.91$, $p = 0.06$, Cohen's $d = 0.55$
Decoding onset	222.10 ± 72.59 ms	219.6 ± 66.18 ms	$t_{(37)} = 0.11$, $p = 0.91$, Cohen's $d = 0.03$
Target-locked diagonal decoding (all electrodes); small cue trials based on target eccentricity (2 vs. 12°)			
Key decoding measures	**ASD (paired-sample *t*-test)**	**TD (paired-sample *t*-test)**	**ASD versus TD between comparisons (*p*-value, independent sample *t*-test)**
Classification accuracy (AUC)	136–496 ms $p < 0.001$ (cluster-based permutation)***	188–496 ms $p < 0.001$ (cluster-based permutation)***	144–196 ms $p = 0.024$ (cluster-based permutation)*
Decoding sustainability	60.27 ± 4.6%	56.95 ± 4.09%	$t_{(37)} = 2.35$, $p = 0.024$, Cohen's $d = 0.755$*
Decoding peak amplitude	72.14 ± 0.06 (AUC)	67.73 ± 0.05 (AUC)	$t_{(37)} = 2.45$, $p = 0.019$, Cohen's $d = 0.78$*
Decoding peak latency	295.78 ± 110.64 ms	359.6 ± 100.64 ms	$t_{(37)} = -1.88$, $p = 0.09$, Cohen's $d = -0.6$
Decoding onset	237.05 ± 74.01 ms	280.2 ± 83.22 ms	$t_{(37)} = -1.70$, $p = 0.96$, Cohen's $d = -0.54$

Note: The asterisks indicate the significant difference: *$p < 0.05$; **$p < 0.01$; ***$p < 0.001$.

performed statistical comparisons for each ROI analyzed (i.e., independent sample t-tests). In detail, we aimed to probe the potential differences between ASD and TD groups revealed by within-group analysis, thus comparing the cue-related decoding activity in the time window after the target onset for each ROI (i.e., 500–998 ms). This analysis revealed a higher and sustained decoding of cue-related neural activity in ASD with respect to TD group on left posterior ($t_{(37)} = 2.453$, $p = 0.019$, Cohen's $d = 0.786$; ASD: 0.557 ± 0.020%; TD: 0.539 ± 0.029) and central ($t_{(37)} = 2.031$, $p = 0.049$, Cohen's $d = 0.651$; ASD: 0.538 ± 0.013%; TD: 0.525 ± 0.025) clusters, supporting the hypothesis of a sustained and greater diffuse diagonal decoding on ASD as compared to TD group (see Table 2 for detailed results description).

In addition, we computed cluster-based corrected permutations t-tests on the entire cue-locked time window (0–998 ms) to evaluate statistical differences in AUC between ASD and TD groups for each ROI; this analysis did not show statistically significant differences ($p > 0.05$).

Decoding large versus small trials: MVPA – temporal generalization

Since cue-locked diagonal decoding revealed that ASD group, when compared to TD group, showed a sustained decoding of cue-locked response even after the target onset, it was conceivable that the observed cue-locked neural response was generalized even after the target onset (500 ms).

For both ASD and TD groups, this analysis revealed that training the classifier at a given time point effectively generalized across a range of time points (Figure 3a; see Table 2 for detailed results description). However, for the ASD group cue decoding showed a broader window of generalization when compared to the TD group, revealing a significant generalized neural pattern associated with cue information processing even after the target onset (observed significant cluster: 156–998 ms, $p < 0.001$; Figure 3a). However, when we computed permutation tests with cluster-based correction between

19393806, 2024, 1, Downloaded from https://onlinelibrary.wiley.com/doi/10.1002/aur.3062 by CochraneItalia, Wiley Online Library on [07/07/2024]. See the Terms and Conditions (https://onlinelibrary.wiley.com/terms-and-conditions) on Wiley Online Library for rules of use; OA articles are governed by the applicable Creative Commons License

ASD and TD groups, such analysis did not show statistically significant differences ($p > 0.05$).

To evaluate these differences more deeply, we trained the classifier on the time range around the peak of the neural code decoded on diagonal analysis, separately for ASD (peak accuracy: 156 ms – trained on 106–206 ms) and TD groups (peak accuracy: 168 ms – trained on 118–218 ms). In other words, we have identified the cue-related neural pattern separately for ASD and TD groups (ASD = 106–206 ms; TD = 118–218 ms), separately evaluating whether the resulting neural code generalizes over cue-locked time window (Figure 3b). Results showed that only the ASD group exhibited a generalized neural pattern over the entire time window, and thus even after the target onset, (ASD: 108–998 ms, $p < 0.001$), contrarily to the TD group whose neural code expires at the target onset (TD: 112–491 ms, $p < 0.001$), suggesting a difficulty in the ASD group in disengaging attentional resources from the current state (i.e., cue processing) and shift to a new stimulus processing (i.e., target processing).

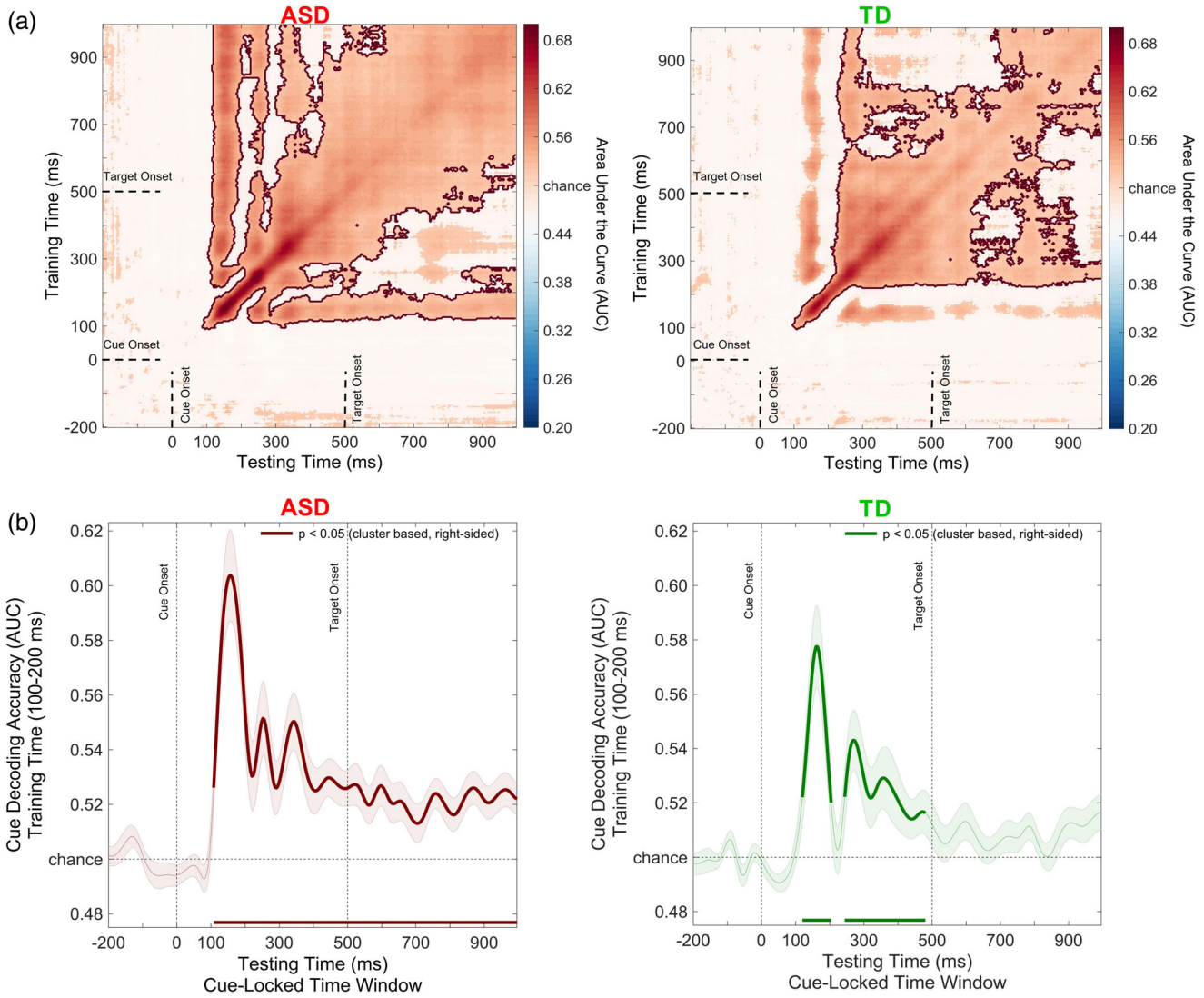

FIGURE 3 (a) Large versus small cue trials time generalization analysis trained and tested on the cue-locked time window (−200 to 998 ms). Results showed that training the classifier at a given timepoint generalized across a range of timepoints (e.g., statistically significant timepoints are outlined in dark red) for both ASD (left panel) and TD (right panel) groups. Such analysis revealed a broader time generalization of the decoded cue-neural code (i.e., decoding peak around 100–200 ms) for the ASD group, showing a recurrent and sustained pattern of generalization even after the target onset (i.e., after 500 ms) only in the ASD group (0 ms = cue onset; 500 ms = onset target). (b) Testing of the cues neural response decoded on the time range around the decoding peak (ASD: 106–206 ms; TD: 118–218 ms) over all timepoints in the cue-locked time window. The results revealed that individuals with ASD (left panel) showed a generalized neural pattern that can be identified even after target onset (500 ms), as opposed to the TD group (right panel). Vertical lines indicated cue appearance (0 ms) and target onset (500 ms). The horizontal line indicates the chance level (50%) against which the performance was tested to judge at which timepoints the decoding was significant (right-sided cluster-based permutation *t*-tests; $p < 0.05$). Shaded areas around bars represent the standard error across participants.

19393806, 2024, 1, Downloaded from https://onlinelibrary.wiley.com/doi/10.1002/aur.3062 by CochraneItalia, Wiley Online Library on [07/07/2024]. See the Terms and Conditions (https://onlinelibrary.wiley.com/terms-and-conditions) on Wiley Online Library for rules of use; OA articles are governed by the applicable Creative Commons License

Decoding target location: Target-locked MVPA

Large cue trials

Regarding decoding of target stimuli based on eccentricity in large cue trials (2° vs. 12°), the cluster-based permutation analysis revealed that classification accuracy (AUC) was sustained significantly above chance level (50%) in both the ASD and TD groups. In detail, the cluster-based permutation analysis revealed a significant decoding of experimental conditions, corresponding to a cluster in the observed data: 144–496 ms for the ASD group, and 132–496 ms for the TD group ($p < 0.001$ for both groups; Figure 4a).

We computed cluster-based permutation corrected t-tests to evaluate statistical differences in AUC between ASD and TD groups; this analysis did not show statistically significant differences ($p > 0.05$; see Figure 4a). Moreover, no significant differences were observed in key decoding measures between the two groups in the target processing based on eccentricity during large cue trials (see Table 2 for detailed results description).

Small cue trials

Regarding decoding of target stimuli based on eccentricity in small cue trials (2° vs. 12°), the cluster-based permutation analysis revealed that classification accuracy (AUC) was sustained significantly above chance level (50%) in both the ASD and TD groups. In detail, the cluster-based permutation analysis showed a significant decoding of experimental conditions, corresponding to a cluster in the observed data: 136–496 ms for the ASD group and 188–496 ms for the TD group ($p < 0.001$ for both groups; see Figure 4b). The decoding accuracy peak

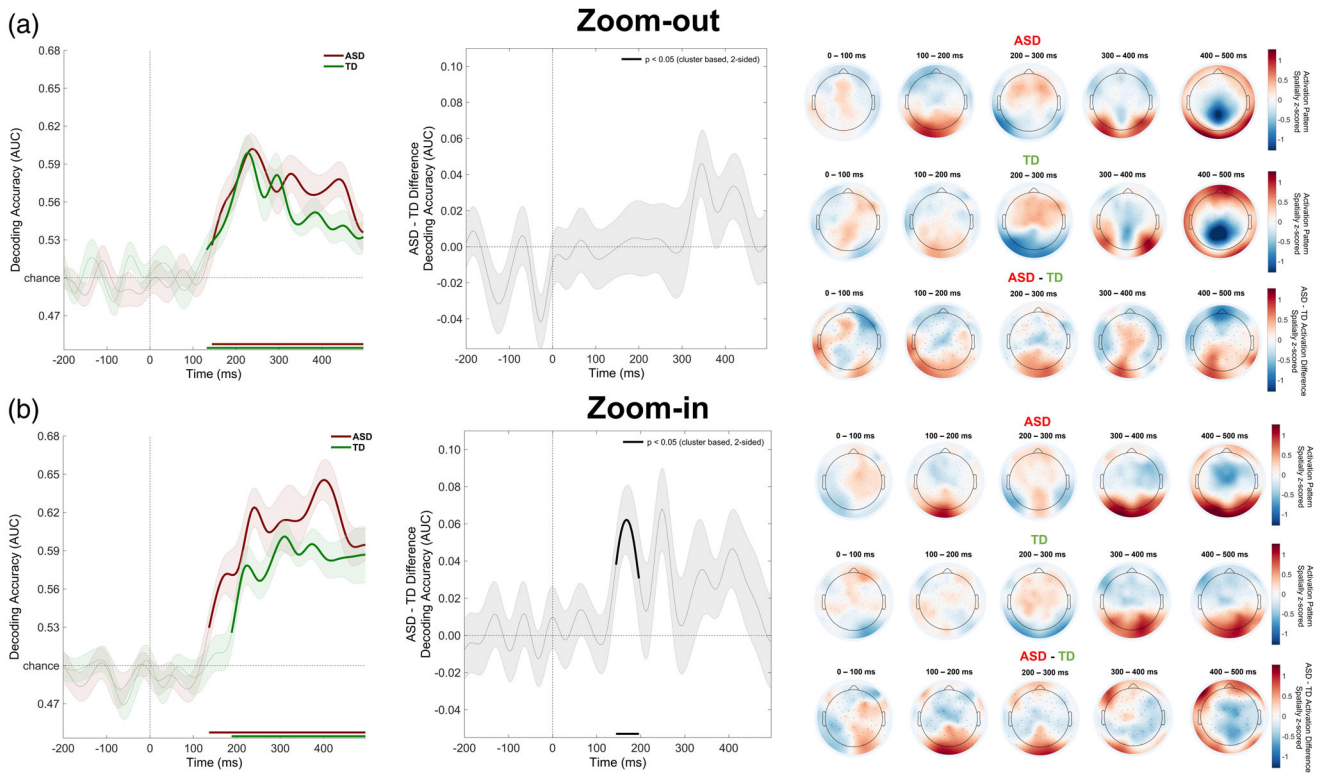

FIGURE 4 Decoding differences of attentional zooming neural dynamics between autism spectrum disorder (ASD) and typically developing (TD) groups (all electrodes). (a) Zoom-out trials. Diagonal decoding of the neural response elicited by the presentation of the visual target at 2° versus 12° from the fixation cross followed by the large cue. The results revealed that the decoding accuracy (AUC) was significantly above chance level (50%) in both the ASD (red line) and TD (green line) groups (left panel), showing no significant differences under this attentional regime between groups (middle panel; two-sided cluster-based permutation test; $p < 0.05$). Activation patterns derived from the product of the weight vectors and the covariance matrix for individual features (electrodes) over target-locked time window during zoom-out trials. The upper, middle, and lower rows show topographic maps of the ASD group, the TD group, and the difference between the two groups, respectively. (b) Small cue trials. Diagonal decoding of the neural response elicited by the presentation of the visual target at 2° versus 12° from the fixation cross followed by the small cue. The results revealed that the decoding accuracy (AUC) was significantly above chance level (50%) in both the ASD (red line) and TD (green line) groups (left panel). In this visual attentional condition, the decoding accuracy onset emerges earlier in the ASD group as compared to the TD group, showing significant differences between groups in a cluster of the observed data beginning at 140 ms and ending at 200 ms (middle panel; both-sided cluster-based permutation test, $p < 0.05$). Activation patterns derived from the product of the weight vectors and the covariance matrix for individual features (electrodes) over target-locked time window during small cue trials. The upper, middle and lower rows show topographic maps of the ASD group, the TD group, and the difference between the two groups, respectively.

19393806, 2024, 1, Downloaded from https://onlinelibrary.wiley.com/doi/10.1002/aur.3062 by CochraneItalia, Wiley Online Library on [07/07/2024]. See the Terms and Conditions (https://onlinelibrary.wiley.com/terms-and-conditions) on Wiley Online Library for rules of use; OA articles are governed by the applicable Creative Commons License

after cue onset achieved by the ASD group emerges later than in the TD group (ASD: 392 ms; TD: 312 ms), with the ASD group reaching a higher level in the peak of decoding accuracy (64.90%) compared to the TD group (60.60%).

We implemented cluster-based permutation corrected t-tests to evaluate statistical differences in AUC between ASD and TD groups; this analysis showed a difference between groups ($p = 0.024$); Figure 4b), corresponding to a cluster in the observed data beginning at 144 ms and ending at 196 ms. This result reflects an earlier decoding onset of target eccentricity in small cue trials in the ASD group with respect to the TD group.

Finally, as already implemented in small cue trials, we compared decoding measures at the individual participants level between the two groups; we found significant differences in the decoding peak ($t_{(37)} = 2.45$, $p = 0.019$, Cohen's $d = 0.78$; ASD: 0.72 ± 0.06; TD: 0.67 ± 0.05) and decoding sustainability ($t_{(37)} = 2.35$, $p = 0.024$, Cohen's $d = 0.755$; ASD: 60.27 ± 4.6%; TD: 56.95 ± 4.09%; see Table 2 for detailed results description). Overall, these results suggest an aberrant hyper-focused visual spatial attention in the ASD group, reflected by an early onset and a delayed decoding peak of decoding relative to the TD group.

Correlation between large versus small cue trials decoding and behavioral measures

Based on cue-locked decoding results (i.e., large vs. small cue trials), we hypothesized that the sustained decoding of the cue-related neural activity detected after target onset might affect the ability to zoom-in and/or zoom-out the focus of visual attention in the ASD group. In line with this prediction, the correlation analysis revealed that sustained decoding of the cue after target onset correlated positively with the RTs of the small cue-trials when target were present peripherally at eccentricity 12 ($r = 0.687$, $p < 0.001$) in the ASD group, but not in the TD group ($r = -0.175$, $p = 0.46$; Figure 5). For both groups, no further significant correlations emerged in the other conditions (all ps >0.298).

Univariate ERPs results

Differently from MVPA, univariate analysis performed separately on the mean amplitude and peak latency of P1 and N1 ERPs components did not reveal significant differences between experimental groups (ASD vs. TD), both in cue- and target-locked time windows (see cue- and target-locked results, respectively, in Figures 6 and 7; for a more detailed description, see supplementary), strengthening the idea that MVPA analysis of EEG data might be more sensitive in revealing hidden neural dynamics which may remain largely blind to classical univariate analysis techniques.

DISCUSSION

The main purpose of the current study was to explore the neural dynamics underlying visuo-attentional dysfunctions in children with ASD implementing a state-of-the-art MVPA approach of EEG data acquired during an attentional zooming task, where according to previous behavioral reports individuals with ASD show a hyperfocused visuo-attentional profile (Mann & Walker, 2003; Ronconi et al., 2012, 2013, 2018; Robertson et al., 2017). MVPA allowed us to highlight different signatures of atypical neural patterns during the exogenous modulation of the visuo-spatial attentional focus in children with ASD, showing an atypical hyper-focusing of visual attentional resources that emerged both during the cue and target processing.

First, our findings showed that cue-locked activity, as shown by decoding of large versus small cue neural responses, required a higher allocation of neural resources (e.g., Bae et al., 2020) in the ASD group when compared to the TD group. When looking at the diagonal decoding of the cue-size neural response, both ASD and TD groups showed a sustained significant decoding of neural activity after cue onset, with the highest decoding accuracy observed in the central-posterior ROI. Furthermore, in both experimental groups, cue-locked neural responses have been significantly decoded in other different scalp areas comprising posterior, central, and anterior regions. This is in line with the evidence demonstrating that visuo-spatial attentional mechanisms may be orchestrated globally by different brain networks and regions, with a paramount role of top-down fronto-parietal attentional networks (Belmonte et al., 2010; Corbetta & Shulman, 2002; Saalmann et al., 2007). However, this analysis also revealed that only the ASD group showed a spatially diffuse and sustained significant decoding of the cue-size neural response even after the target onset, potentially suggesting an anomalously broader encoding of the cue information, which was spatially and temporally overrepresented in ASD.

The evidence that a delay in the extinction of neural dynamics associated with the processing of an initial stimulus (in this case, the cue) could potentially interfere with the subsequent processing of other incoming stimuli (in this case, the target) may sheds light on a potential new aspect of dysfunctional neural dynamics underlying visuo-attentional processes in individuals with ASD, and provide new insights for expanding the notion of hyperfocused attention in this population. Indeed, to optimally reorient attention towards incoming stimuli and to correctly perceive globally the relevant information in the visual field (Guy et al., 2019; Happé & Frith, 2006; Ronconi et al., 2013, 2018), there should be a functional reallocation of visuo-attentional resources. Importantly, although our findings did not demonstrate differences between the ASD and TD groups at a behavioral level, to further corroborate our speculations regarding delayed extinction of the neural response associated with the

19393806, 2024, 1, Downloaded from https://onlinelibrary.wiley.com/doi/10.1002/aur.3062 by CochraneItalia, Wiley Online Library on [07/07/2024]. See the Terms and Conditions (https://onlinelibrary.wiley.com/terms-and-conditions) on Wiley Online Library for rules of use; OA articles are governed by the applicable Creative Commons License

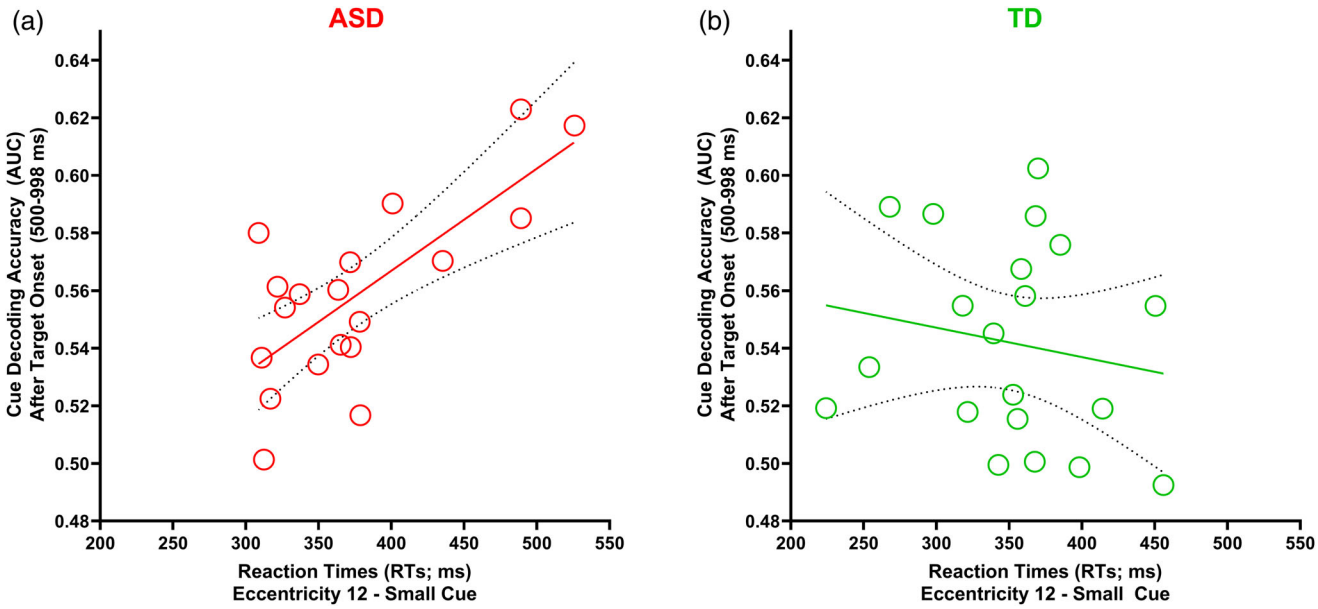

FIGURE 5 The figures highlight the relationships revealed by the Pearson correlation coefficient between the pattern of neural activity (AUC) decoded during the cue-locked time window after target onset (500–998 ms) and the reaction times (RTs) recorded in small cue-trials when target were presented at the peripheral eccentricity (12°), separately for autism spectrum disorder (ASD) (a) and typically developing (TD) (b) groups. A positive association was found only for the ASD group ($p < 0.001$).

processing of the cue potentially interfering with the processing of a visual target, we performed a correlation analysis between the pattern of neural activity elicited by the cue after the target onset, and the ability to zoom-in (small cue trials) and zoom-out (large cue trials) the attentional focus in the two groups as indexed by the behavioral data recorded in our task. This analysis revealed that greater cue processing after the appearance of the target (i.e., higher decoding accuracy) was positively correlated, only in the ASD group, with slower RTs in the condition in which the target was presented peripherally (eccentricity = 12°) following the small cue. In other words, these findings suggest that a sustained processing of the visual information related to the cue after the target appearance in our ASD sample may delay the detection of the subsequent peripheral visual target, thus providing new potential neural bases of their atypical hyper-focused attentional profile and impaired ability to disengage visuo-spatial attention (Burack, 1994; Mann & Walker, 2003; Ronconi et al., 2013, 2018).

To further corroborate this idea, we performed a temporal generalization analysis with cross-classification across time using the activity of all electrodes, in order to probe whether the neural response of the two cue sizes (large vs. small) decoded in the cue-locked time window was sustained and recurring even after the appearance of the target. Intriguingly, only in the ASD group the neural pattern evoked by the cue recurred even after the appearance of the target (500 ms after cue-onset). In detail, the neural response elicited by the cue that could be decoded in the ASD group, showed a sustained temporal generalization even after the appearance of the target, suggesting again an atypical, delayed extinction of the neural response associated with the processing of the cue, whereas in the TD group cue information could not be decoded anymore from this early neural pattern evoked by the cue.

Finally, to investigate the hidden differences in neural dynamics underlying attentional zooming mechanisms between ASD and TD groups, we performed diagonal MVPA decoding of the neural response elicited by the target stimuli as a function of their eccentricity (2° vs. 12°) and attentional requirements (small vs large cue trials). Results revealed significant differences between ASD and TD groups only in the small cue, but not in large cue trials. Specifically, in large cue trials, both ASD and TD groups showed a significant decoding of the neural response elicited by the target based on its eccentricity, and no significant differences between groups emerged in the decoding latency onset and peak accuracy. Contrarily, during small cue trials, although a significant decoding of target eccentricity was again evident in both ASD and TD groups, significant differences in the decoding latency emerged with the ASD group showing an earlier decoding latency onset (132 ms) as compared to the TD group (196 ms). These earlier decoding onsets associated with target processing highlight an atypical pattern of neural activity in small cue trials, supporting previous behavioral evidence demonstrating a prolonged zoom-in attentional focusing in children with ASD (Ronconi et al., 2013, 2018), and more generally the evidence showing attentional anomalies potentially resulting from an atypical hyper-focusing of visuo-spatial attentional resources (Geurts et al., 2009; Ridderinkhof

19393806, 2024, 1, Downloaded from https://onlinelibrary.wiley.com/doi/10.1002/aur.3062 by CochraneItalia, Wiley Online Library on [07/07/2024]. See the Terms and Conditions (https://onlinelibrary.wiley.com/terms-and-conditions) on Wiley Online Library for rules of use; OA articles are governed by the applicable Creative Commons License

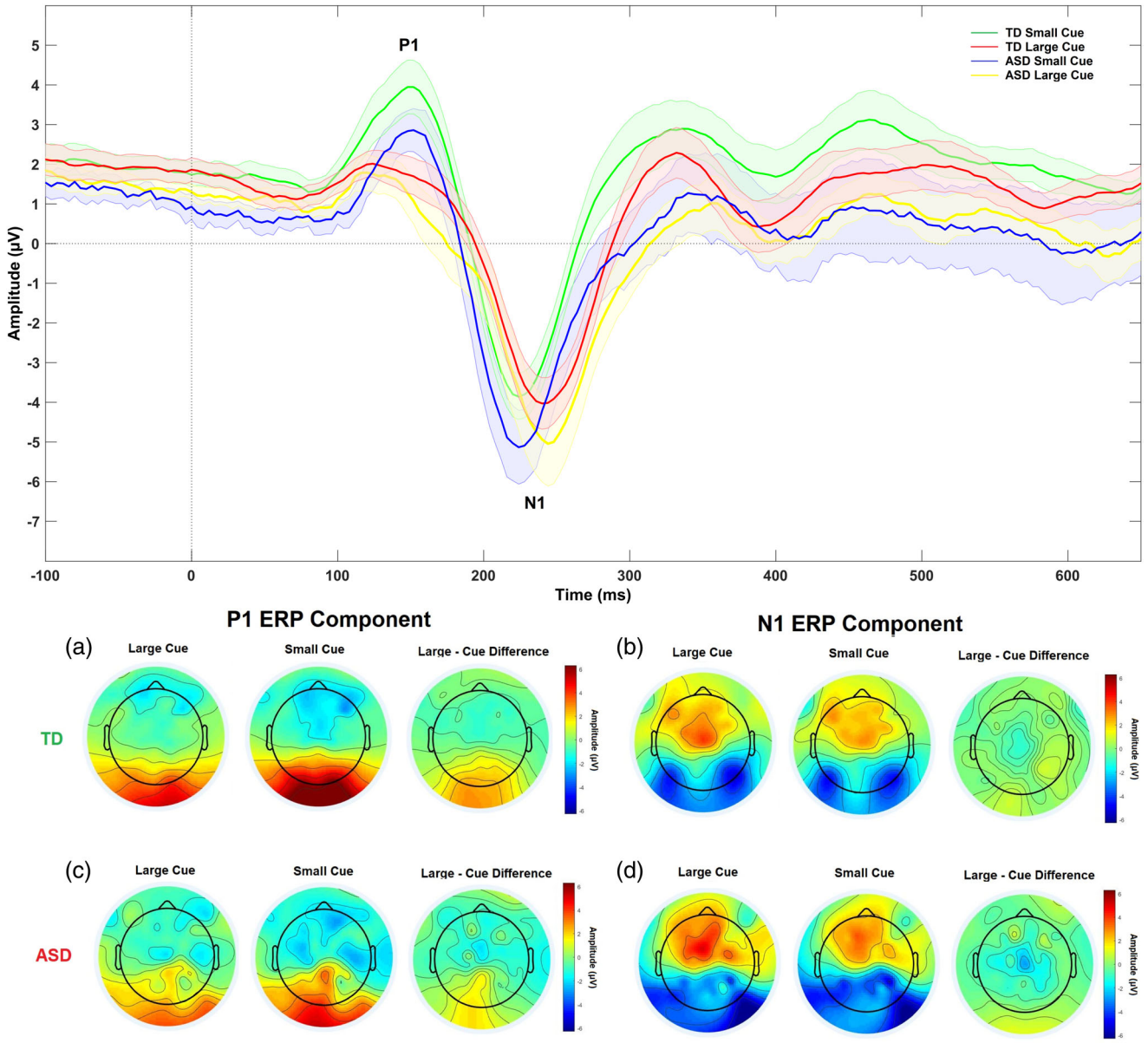

FIGURE 6 Cue-locked ERPs univariate results. ERPs waveforms on central posterior ROI (upper panel) elicited by the small (ASD: blue; TD: green) and large cues (ASD: yellow; TD: red). Univariate ERPs analyses performed on the mean amplitude and peak latency of P1 and N1 ERPs components did not reveal significant differences between experimental groups (ASD vs. TD). Both for P1 and N1 peak latency ($p > 0.334$) and mean amplitude ($p > 0.226$) this analysis did not reveal a significant main effect of the Group and its interaction with other main factors, suggesting no differences between ASD and TD groups. (a) P1 topographical activation maps for the TD group in large (left panel), small (central panel) and their difference (right panel). (b) N1 topographical activation maps for the TD group in large (left panel), small (central panel) and their difference (right panel). (c) P1 topographical activation maps for the ASD group in large (left panel), small (central panel) and their difference (right panel). (d) N1 topographical activation maps for the ASD group in large (left panel), small (central panel) and their difference (right panel).

et al., 2020). Furthermore, in small cue trials, children with ASD showed a higher decoding peak accuracy when compared to the TD group. This result emerged even though the ASD group showed the peak of their decoding accuracy at a significantly delayed neural timing after target onset as compared to the TD group. This delayed peak accuracy shown by children with ASD might suggest sluggish target information processing during zoom-in condition, potentially resulting from the hyper-focusing of visuo-attentional resources during cue processing, and thus being a potential source of interference to the processing of the incoming target stimulus.

Hence, we may speculate that the higher decoding peak shown by individuals with ASD with respect to TD group could reflect a dysfunctional processing of perceptual information, leading to an atypical hyper-focusing of visuo-spatial attentional resources. We have advanced the speculation that higher decoding peak shown by individuals with ASD with respect to TD group, both on the cue and target-locked period, could reflect a

19393806, 2024, 1, Downloaded from https://onlinelibrary.wiley.com/doi/10.1002/aur.3062 by CochraneItalia, Wiley Online Library on [07/07/2024]. See the Terms and Conditions (https://onlinelibrary.wiley.com/terms-and-conditions) on Wiley Online Library for rules of use; OA articles are governed by the applicable Creative Commons License

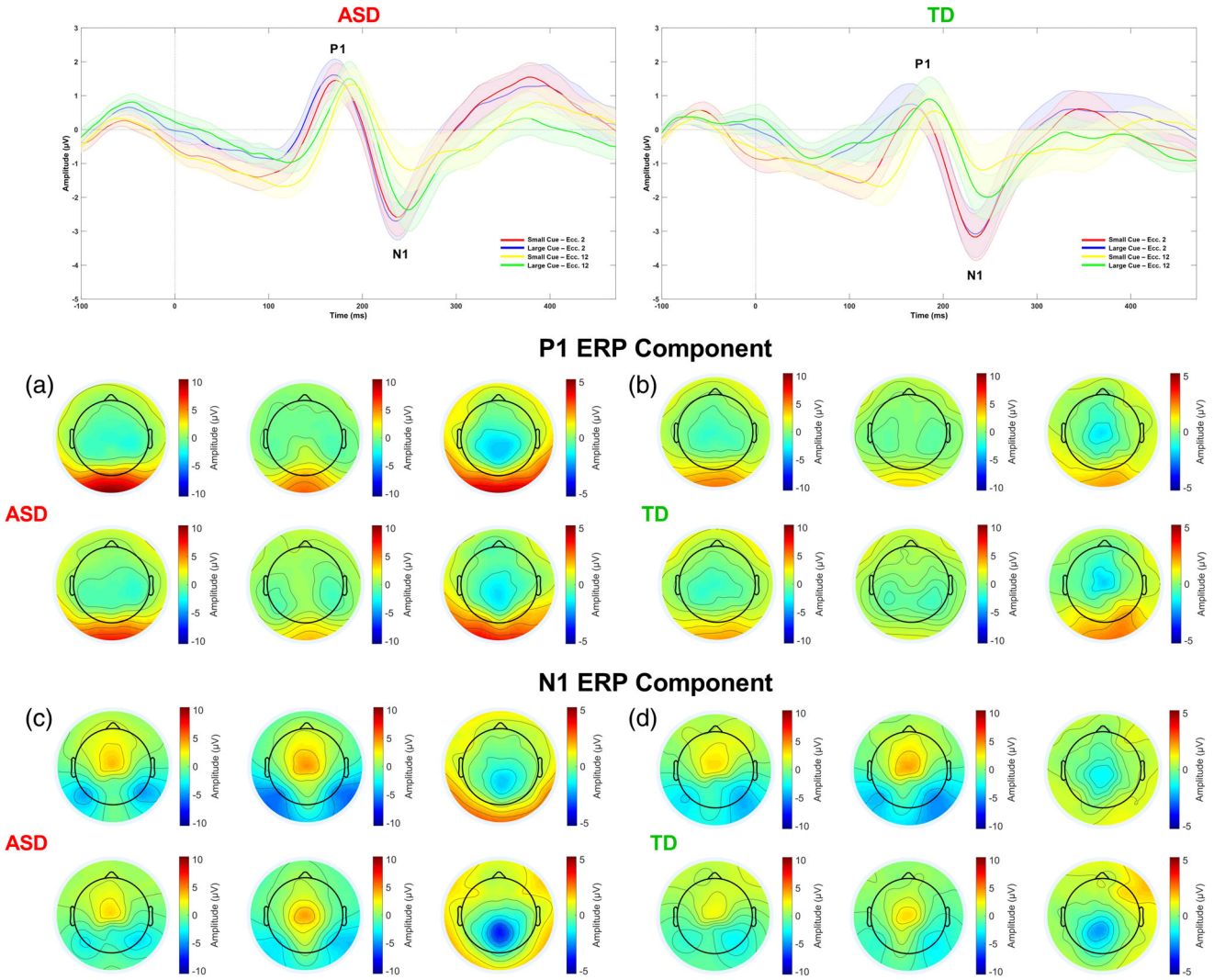

FIGURE 7 Target-locked ERPs univariate results. ERPs waveforms on central posterior ROI (upper panel) elicited by the visual target at the eccentricity 2 and 12 as a function of the focusing cue-size (zoom-in and zoom-out trials) for each experimental group (ASD and TD). Univariate target-locked ERPs analyses performed on P1 and N1 peak latency ($p > 0.45$) and mean amplitude ($p > 0.26$) did not reveal significant main effects of group and its interaction with other main factors, suggesting no differences between ASD and TD groups. (a) P1 topographical activation maps for the ASD group in zoom-out trials (left panel), in zoom-in trials (central panel) and their difference (right panel). (b) P1 topographical activation maps for the TD group in zoom-out trials (left panel), in zoom-in trials (central panel) and their difference (right panel). (c) N1 topographical activation maps for the ASD group in zoom-out trials (left panel), in zoom-in trials (central panel) and their difference (right panel). (d) N1 topographical activation maps for the TD group in zoom-out trials (left panel), in zoom-in trials (central panel) and their difference (right panel).

dysfunctional processing of perceptual information linked to an atypical hyper-focusing of visuo-spatial attention. Intriguingly, a previous study in individuals with schizophrenia (SCZ) has come to a similar conclusion. Bae et al. (2020) implemented MVPA of EEG data in a sample of patients with SCZ, with the aim of investigating the neural dynamics differences in visual working memory processes when compared to TD population. They found a greater decoding accuracy of different experimental conditions in individuals with SCZ, suggesting that such findings might reflect the aberrant hyperfocusing of cognitive resources, according to the hyperfocusing hypothesis of SCZ (Bae et al., 2020; Luck et al., 2019). Similarly, we hypothesize that the sensory profile typically exhibited by individuals with ASD, often characterized by a pervaded feeling of sensory overload (Grandin, 2009; Belmonte et al., 2010; Kern et al., 2006; Baruth et al., 2010; Ronconi et al., 2018; Parmar et al., 2021), could be linked to an atypical and excessive automatic attentional capture of sensory inputs, with a consequent difficulty to disengage their attentional resources, preventing the extinction of information processing and delaying the processing of incoming relevant stimuli. However, in the absence of further combined MVPA-EEG and behavioral evidence such interpretations remain merely speculative.

19393806, 2024, 1, Downloaded from https://onlinelibrary.wiley.com/doi/10.1002/aur.3062 by CochraneItalia, Wiley Online Library on [07/07/2024]. See the Terms and Conditions (https://onlinelibrary.wiley.com/terms-and-conditions) on Wiley Online Library for rules of use; OA articles are governed by the applicable Creative Commons License

LIMITATIONS

As the first application of the MVPA technique to investigate visuo-attentional dysfunctions in children with ASD, our study is not exempt from methodological and conceptual limitations.

Indeed, although MVPA analyses revealed differences between groups in the exogenous processing of visual stimuli during the cue-target period, the behavioral results, despite highlighting an effective influence of the attentional conditions (small cue vs. large cue trials) on the overall pattern of RTs, did not revealed RTs differences between TD and ASD groups, differently from previous evidence (Ronconi et al., 2012, 2013, 2018). Among the factors that can explain this null effect, it is important to consider that here we used only a fixed cue-target SOA at 500 ms. Previous evidence demonstrated differences in children with ASD at shorter SOA (i.e., 100 ms), since longer SOAs might be too long to elicit a clear modulation of RTs in attentional focusing task (Ronconi et al., 2013; Turatto et al., 2000).

Relatedly, another potential explanation may rely on the choice of including a smaller portion of trials with shorter SOA, with the aim to reduce potential prediction-related issues (e.g., Ronconi et al., 2023), and more generally to induce a less strong expectation about the timing of target onset, avoiding a strong prediction about the timing of target appearance. At the theoretical level, there is the possibility that some of the differences between ASD and TD groups highlighted in the present study also arises due to the putative anomalies in forming predictions in individuals with ASD (e.g., Ronconi et al., 2023), although we could not directly probe this hypothesis in the current study, since the analyses were limited selectively to the 500 ms SOA condition, where enough trials were available to compute EEG data analysis.

Another important methodological limitation of the current study concerns the absence of eye-tracking instrumentation aimed at investigating the maintenance of fixation and of potential eye movements during our visuospatial attention task. Although we may be confident that our strategy of verifying the maintenance of fixation through EOG artifacts present in the EEG signal may have limited potential spurious effect, future research incorporating eye-tracking techniques is desirable.

In addition, a further critical issue arises from the impossibility of disambiguating whether in the current study the MVPA differences identified between the TD and ASD groups reflect cue stimulation differences rather than visuo-spatial attentional mechanisms modulation.

Finally, the limited sample of participants with ASD tested in the present study does not allow us to generalize our findings to the entire autism spectrum. MVPA is an analysis typically linked to systematic biases in contexts in which data sample distributions are small, a criticality that emerges with greater emphasis in the case of ASD, a neurodevelopmental disorder characterized by high heterogeneity and peculiarities of the individual neurodevelopmental trajectories (e.g., Elsabbagh et al., 2011; Mazer, 2011). To limit potential biases arising from the MVPA analysis, we decided to use a non-parametric measure (AUC) for our analyses, which has been proven to be an accurate measure of generalization in these situations (King & Dehaene, 2014; López-García et al., 2020). However, the ASD sample of this study was characterized by average or above average IQ and did not have ADHD, thus representing only a narrow phenotype within the spectrum. Hence, future studies can explore whether such anomalies identified in our sample are generalizable to a broader ASD population, for example with below average IQ, leaving the chance to explore whether this neural encoding pattern is effectively responsible for visuo-attentional key deficits in a large portion of individuals with ASD.

CONCLUSIONS

To sum up, the present study represents the first attempt to use MVPA of EEG data in order to make inferences about the flow of visual information processing under different attentional conditions in ASD. Such innovative approach allowed us to describe how incoming visual input are encoded at the neural level in children with ASD, showing that in both the cue- and target-locked time windows, the hyperfocused attention that has consistently been associated to ASD (Geurts et al., 2009; Isomura et al., 2015; Ridderinkhof et al., 2020), may be linked at the neural level to an overrepresentation of stimulus information. We suggest that this excessive stimulus encoding, which we found to persist for longer time and to involve broader brain regions, could in turn lead to difficulties in disengaging and reorienting attentional resources to subsequent relevant incoming stimuli.

AUTHOR CONTRIBUTIONS

Conceptualization: Gianluca Marsicano, Luca Casartelli, Andrea Facoetti, Luca Ronconi. Investigation: Luca Casartelli, Alessandra Federici, Sara Bertoni, Lorenzo Vignali, Massimo Molteni. Contributed analytic tools: Gianluca Marsicano, Lorenzo Vignali, Luca Ronconi. Analyzed data: Gianluca Marsicano, Luca Casartelli, Alessandra Federici, Luca Ronconi. Supervision: Luca Casartelli, Andrea Facoetti, Luca Ronconi. Resources: Luca Casartelli, Massimo Molteni. Visualization: Gianluca Marsicano. Wrote the paper (original draft preparation): Gianluca Marsicano, Luca Ronconi. Wrote the paper (reviewing and editing): Luca Casartelli, Alessandra Federici, Sara Bertoni, Lorenzo Vignali, Massimo Molteni, Andrea Facoetti.

ACKNOWLEDGMENTS

We thank all the children and their parents who participated in our study. Open access funding provided by BIBLIOSAN.

19393806, 2024, 1, Downloaded from https://onlinelibrary.wiley.com/doi/10.1002/aur.3062 by CochraneItalia, Wiley Online Library on [07/07/2024]. See the Terms and Conditions (https://onlinelibrary.wiley.com/terms-and-conditions) on Wiley Online Library for rules of use; OA articles are governed by the applicable Creative Commons License

FUNDING INFORMATION
This research did not receive any specific grant from funding agencies in the public, commercial, or not-for-profit sectors.

CONFLICT OF INTEREST STATEMENT
The authors declare no conflict of interest.

DATA AVAILABILITY STATEMENT
The data that support the findings of this study are available on request from the corresponding author. The data are not publicly available due to privacy or ethical restrictions.

ETHICS STATEMENT
The entire research protocol was approved by the ethics committees of the I.R.C.C.S. "E. Medea". Informed consent was obtained from each child and their parents. The research was conducted according to the principles set out in the Declaration of Helsinki.

ORCID
Gianluca Marsicano https://orcid.org/0000-0001-6216-4404
Luca Casartelli https://orcid.org/0000-0002-8528-4510
Alessandra Federici https://orcid.org/0000-0002-7840-5273
Sara Bertoni https://orcid.org/0000-0002-0985-0373
Massimo Molteni https://orcid.org/0000-0001-6268-5883
Andrea Facoetti https://orcid.org/0000-0002-4626-6213
Luca Ronconi https://orcid.org/0000-0002-4674-8917

REFERENCES
American Psychiatric Association. (1994). *Diagnostic and statistical manual of mental disorders (DSM-IV®)*. American Psychiatric Association.

Bae, G. Y., Leonard, C. J., Hahn, B., Gold, J. M., & Luck, S. J. (2020). Assessing the information content of ERP signals in schizophrenia using multivariate decoding methods. *NeuroImage: Clinical*, *25*, 102179.

Bara, B. G., Bucciarelli, M., & Colle, L. (2001). Communicative abilities in autism: Evidence for attentional deficits. *Brain and Language*, *77*(2), 216–240.

Baruth, J., Casanova, M., Sears, L., & Sokhadze, E. (2010). Early-stage visual processing abnormalities in high-functioning autism spectrum disorder (ASD). *Translational Neuroscience*, *1*(2), 177–187.

Battistoni, E., Kaiser, D., Hickey, C., & Peelen, M. V. (2020). The time course of spatial attention during naturalistic visual search. *Cortex*, *122*, 225–234.

Belmonte, M. K., Gomot, M., & Baron-Cohen, S. (2010). Visual attention in autism families: 'unaffected'sibs share atypical frontal activation. *Journal of Child Psychology and Psychiatry*, *51*(3), 259–276.

Burack, J. A. (1994). Selective attention deficits in persons with autism: Preliminary evidence of an inefficient attentional lens. *Journal of Abnormal Psychology*, *103*(3), 535–543.

Corbetta, M., & Shulman, G. L. (2002). Control of goal-directed and stimulus-driven attention in the brain. *Nature Reviews Neuroscience*, *3*(3), 201–215.

Delorme, A., & Makeig, S. (2004). EEGLAB: An open source toolbox for analysis of single-trial EEG dynamics including independent component analysis. *Journal of Neuroscience Methods*, *134*(1), 9–21.

Elsabbagh, M., Holmboe, K., Gliga, T., Mercure, E., Hudry, K., Charman, T., & BASIS Team. (2011). Social and attention factors during infancy and the later emergence of autism characteristics. *Progress in Brain Research*, *189*, 195–207.

Fahrenfort, J. J., Grubert, A., Olivers, C. N., & Eimer, M. (2017). Multivariate EEG analyses support high-resolution tracking of feature-based attentional selection. *Scientific Reports*, *7*(1), 1886.

Fahrenfort, J. J., van Driel, J., van Gaal, S., & Olivers, C. N. (2018). From ERPs to MVPA using the Amsterdam decoding and modeling toolbox (ADAM). *Frontiers in Neuroscience*, *12*, 368.

Farran, E. K., & Karmiloff-Smith, A. (Eds.). (2011). *Neurodevelopmental disorders across the lifespan: A neuroconstructivist approach*. OUP Oxford.

Farran, E. K., Mares, I., Papasavva, M., Smith, F. W., Ewing, L., & Smith, M. L. (2020). Characterizing the neural signature of face processing in Williams syndrome via multivariate pattern analysis and event related potentials. *Neuropsychologia*, *142*, 107440.

Fu, S., Caggiano, D. M., Greenwood, P. M., & Parasuraman, R. (2005). Event-related potentials reveal dissociable mechanisms for orienting and focusing visuospatial attention. *Cognitive Brain Research*, *23*(2–3), 341–353.

Geurts, H. M., Corbett, B., & Solomon, M. (2009). The paradox of cognitive flexibility in autism. *Trends in Cognitive Sciences*, *13*(2), 74–82.

Grandin, T. (2009). Visual abilities and sensory differences in a person with autism. *Biological Psychiatry*, *65*(1), 15–16.

Grootswagers, T., Wardle, S. G., & Carlson, T. A. (2017). Decoding dynamic brain patterns from evoked responses: A tutorial on multivariate pattern analysis applied to time series neuroimaging data. *Journal of Cognitive Neuroscience*, *29*(4), 677–697.

Guy, J., Mottron, L., Berthiaume, C., & Bertone, A. (2019). A developmental perspective of global and local visual perception in autism spectrum disorder. *Journal of Autism and Developmental Disorders*, *49*, 2706–2720.

Happé, F., & Frith, U. (2006). The weak coherence account: Detail-focused cognitive style in autism spectrum disorders. *Journal of Autism and Developmental Disorders*, *36*(1), 5–25.

Haufe, S., Meinecke, F., Görgen, K., Dähne, S., Haynes, J. D., Blankertz, B., & Bießmann, F. (2014). On the interpretation of weight vectors of linear models in multivariate neuroimaging. *NeuroImage*, *87*, 96–110.

Hyman, S. L., Levy, S. E., Myers, S. M., Kuo, D. Z., Apkon, S., Davidson, L. F., & Bridgemohan, C. (2020). Identification, evaluation, and management of children with autism spectrum disorder. *Pediatrics*, *145*(1), e20193447.

Isomura, T., Ogawa, S., Shibasaki, M., & Masataka, N. (2015). Delayed disengagement of attention from snakes in children with autism. *Frontiers in Psychology*, *6*, 241.

Johnson, M. H. (2011). Interactive specialization: A domain-general framework for human functional brain development? *Developmental Cognitive Neuroscience*, *1*(1), 7–21.

Karmiloff-Smith, A. (1998). Development itself is the key to understanding developmental disorders. *Trends in Cognitive Sciences*, *2*(10), 389–398.

Kern, J. K., Trivedi, M. H., Garver, C. R., Grannemann, B. D., Andrews, A. A., Savla, J. S., & Schroeder, J. L. (2006). The pattern of sensory processing abnormalities in autism. *Autism*, *10*(5), 480–494.

King, J. R., & Dehaene, S. (2014). Characterizing the dynamics of mental representations: The temporal generalization method. *Trends in Cognitive Sciences*, *18*(4), 203–210.

Lai, M. C., Anagnostou, E., Wiznitzer, M., Allison, C., & Baron-Cohen, S. (2020). Evidence-based support for autistic people across the lifespan: Maximising potential, minimising barriers, and optimising the person–environment fit. *The Lancet Neurology*, *19*(5), 434–451.

Lawson, R. P., Mathys, C., & Rees, G. (2017). Adults with autism overestimate the volatility of the sensory environment. *Nature Neuroscience*, *20*(9), 1293–1299.

19393806, 2024, 1, Downloaded from https://onlinelibrary.wiley.com/doi/10.1002/aur.3062 by CochraneItalia, Wiley Online Library on [07/07/2024]. See the Terms and Conditions (https://onlinelibrary.wiley.com/terms-and-conditions) on Wiley Online Library for rules of use; OA articles are governed by the applicable Creative Commons License

Li, D., Luo, X., Guo, J., Kong, Y., Hu, Y., Chen, Y., & Song, Y. (2023). Information-based multivariate decoding reveals imprecise neural encoding in children with attention deficit hyperactivity disorder during visual selective attention. *Human Brain Mapping*, *44*(3), 937–947.

Lieder, I., Adam, V., Frenkel, O., Jaffe-Dax, S., Sahani, M., & Ahissar, M. (2019). Perceptual bias reveals slow-updating in autism and fast-forgetting in dyslexia. *Nature Neuroscience*, *22*(2), 256–264.

López-García, D., Sobrado, A., Peñalver, J. M., Górriz, J. M., & Ruz, M. (2020). Multivariate pattern analysis techniques for electroencephalography data to study flanker interference effects. *International Journal of Neural Systems*, *30*(7), 2050024.

Lord, C., Rutter, M., DiLavore, P., & Risi, S. (2002). *Autism diagnostic observation schedule*. ADOS Western Psychological Services.

Luck, S. J., Hahn, B., Leonard, C. J., & Gold, J. M. (2019). The hyperfocusing hypothesis: A new account of cognitive dysfunction in schizophrenia. *Schizophrenia Bulletin*, *45*(5), 991–1000.

Luo, Y. J., Greenwood, P. M., & Parasuraman, R. (2001). Dynamics of the spatial scale of visual attention revealed by brain event-related potentials. *Cognitive Brain Research*, *12*(3), 371–381.

Mann, T. A., & Walker, P. (2003). Autism and a deficit in broadening the spread of visual attention. *Journal of Child Psychology and Psychiatry*, *44*(2), 274–284.

Mares, I., Ewing, L., Farran, E. K., Smith, F. W., & Smith, M. L. (2020). Developmental changes in the processing of faces as revealed by EEG decoding. *NeuroImage*, *211*, 116660.

Maris, E., & Oostenveld, R. (2007). Nonparametric statistical testing of EEG-and MEG-data. *Journal of Neuroscience Methods*, *164*(1), 177–190.

Marti, S., & Dehaene, S. (2017). Discrete and continuous mechanisms of temporal selection in rapid visual streams. *Nature Communications*, *8*(1), 1955.

Masi, A., DeMayo, M. M., Glozier, N., & Guastella, A. J. (2017). An overview of autism spectrum disorder, heterogeneity and treatment options. *Neuroscience Bulletin*, *33*, 183–193.

Mazer, J. A. (2011). Spatial attention, feature-based attention, and saccades: Three sides of one coin? *Biological Psychiatry*, *69*(12), 1147–1152.

Mitra, P. P., & Pesaran, B. (1999). Analysis of dynamic brain imaging data. *Biophysical Journal*, *76*(2), 691–708.

Moerel, D., Grootswagers, T., Robinson, A. K., Shatek, S. M., Woolgar, A., Carlson, T. A., & Rich, A. N. (2022). The time-course of feature-based attention effects dissociated from temporal expectation and target-related processes. *Scientific Reports*, *12*(1), 6968.

Mottron, L., Dawson, M., Soulières, I., Hubert, B., & Burack, J. (2006). Enhanced perceptual functioning in autism: An update, and eight principles of autistic perception. *Journal of Autism and Developmental Disorders*, *36*, 27–43.

Munneke, J., Fahrenfort, J. J., Sutterer, D., Theeuwes, J., & Awh, E. (2021). Multivariate analysis of EEG activity indexes contingent attentional capture. *NeuroImage*, *226*, 117562.

Noel, J. P., Zhang, L. Q., Stocker, A. A., & Angelaki, D. E. (2021). Individuals with autism spectrum disorder have altered visual encoding capacity. *PLoS Biology*, *19*(5), e3001215.

Parmar, K. R., Porter, C. S., Dickinson, C. M., Pelham, J., Baimbridge, P., & Gowen, E. (2021). Visual sensory experiences from the viewpoint of autistic adults. *Frontiers in Psychology*, *12*, 633037.

Poldrack, R. A. (2006). Can cognitive processes be inferred from neuroimaging data? *Trends in Cognitive Sciences*, *10*(2), 59–63.

Poldrack, R. A. (2011). Inferring mental states from neuroimaging data: From reverse inference to large-scale decoding. *Neuron*, *72*(5), 692–697.

Ridderinkhof, A., de Bruin, E. I., van den Driesschen, S., & Bögels, S. M. (2020). Attention in children with autism spectrum disorder and the effects of a mindfulness-based program. *Journal of Attention Disorders*, *24*(5), 681–692.

Robertson, C. E., & Baron-Cohen, S. (2017). Sensory perception in autism. *Nature Reviews Neuroscience*, *18*(11), 671–684.

Ronconi, L., Gori, S., Federici, A., Devita, M., Carna, S., Sali, M. E., & Facoetti, A. (2018). Weak surround suppression of the attentional focus characterizes visual selection in the ventral stream in autism. *NeuroImage: Clinical*, *18*, 912–922.

Ronconi, L., Gori, S., Ruffino, M., Franceschini, S., Urbani, B., Molteni, M., & Facoetti, A. (2012). Decreased coherent motion discrimination in autism spectrum disorder: The role of attentional zoom-out deficit. *PLoS One*, *7*(11), e49019.

Ronconi, L., Gori, S., Ruffino, M., Molteni, M., & Facoetti, A. (2013). Zoom-out attentional impairment in children with autism spectrum disorder. *Cortex*, *49*(4), 1025–1033.

Ronconi, L., Vitale, A., Federici, A., Mazzoni, N., Battaglini, L., Molteni, M., & Casartelli, L. (2023). Neural dynamics driving audio-visual integration in autism. *Cerebral Cortex*, *33*(3), 543–556.

Ruff, C. C., Bestmann, S., Blankenburg, F., Bjoertomt, O., Josephs, O., Weiskopf, N., & Driver, J. (2008). Distinct causal influences of parietal versus frontal areas on human visual cortex: Evidence from concurrent TMS–fMRI. *Cerebral Cortex*, *18*(4), 817–827.

Saalmann, Y. B., Pigarev, I. N., & Vidyasagar, T. R. (2007). Neural mechanisms of visual attention: How top-down feedback highlights relevant locations. *Science*, *316*(5831), 1612–1615.

Sinnott-Armstrong, W., & Simmons, C. (2021). Some common fallacies in arguments from M/EEG data. *NeuroImage*, *245*, 118725.

Song, W. Q., Li, X., Luo, Y. J., Du, B. Q., & Ji, X. M. (2006). Brain dynamic mechanisms of scale effect in visual spatial attention. *Neuroreport*, *17*(15), 1643–1647.

Turatto, M., Benso, F., Facoetti, A., Galfano, G., Mascetti, G. G., & Umiltà, C. (2000). Automatic and voluntary focusing of attention. *Perception & Psychophysics*, *62*, 935–952.

Uljarević, M., Baranek, G., Vivanti, G., Hedley, D., Hudry, K., & Lane, A. (2017). Heterogeneity of sensory features in autism spectrum disorder: Challenges and perspectives for future research. *Autism Research*, *10*(5), 703–710.

Wechsler, D. (1993). Scala di Intelligenza Wechsler per Bambini Riveduta (WISC-R).

Zhang, Q., Liang, T., Zhang, J., Fu, X., & Wu, J. (2018). Electrophysiological evidence for temporal dynamics associated with attentional processing in the zoom lens paradigm. *PeerJ*, *6*, e4538.

SUPPORTING INFORMATION

Additional supporting information can be found online in the Supporting Information section at the end of this article.

How to cite this article: Marsicano, G., Casartelli, L., Federici, A., Bertoni, S., Vignali, L., Molteni, M., Facoetti, A., & Ronconi, L. (2024). Prolonged neural encoding of visual information in autism. *Autism Research*, *17*(1), 37–54. https://doi.org/10.1002/aur.3062

19393806, 2024, 1, Downloaded from https://onlinelibrary.wiley.com/doi/10.1002/aur.3062 by CochraneItalia, Wiley Online Library on [07/07/2024]. See the Terms and Conditions (https://onlinelibrary.wiley.com/terms-and-conditions) on Wiley Online Library for rules of use; OA articles are governed by the applicable Creative Commons License